The fascicular anatomy and peak force capabilities of the sternocleidomastoid muscle

Original communication

Ewan Kennedy[1]

Michael Albert[2]

Helen Nicholson[3]

[1] School of Physiotherapy, University of Otago, Dunedin 9016, New Zealand

[2] Department of Computer Science, University of Otago, Dunedin 9016, New Zealand

[3] Department of Anatomy, University of Otago, Dunedin 9016, New Zealand

Correspondence to: Ewan Kennedy, School of Physiotherapy, University of Otago, Dunedin, New Zealand. Phone: +643 479 5424. Email: ewan.kennedy@otago.ac.nz

Key words: sternocleidomastoid; neck muscles; anatomy; biomechanics

Abstract

Purpose

The fascicular morphology of the sternocleidomastoid (SCM) is not well described in modern anatomical texts, and the biomechanical forces it exerts on individual cervical motion segments are not known. The purpose of this study is to investigate the fascicular anatomy and biomechanics of the SCM combining traditional and modern methods.

Methods

This study is comprised of three parts: Dissection, magnetic resonance imaging (MRI), and biomechanical modelling. Dissection was performed on six embalmed cadavers: three males age 73-74 years; and three females age 63-93 years. The fascicular arrangement and morphologic data were recorded. MRIs were performed on six young, healthy volunteers: three males age 24-37; and three females age 26-28). *In vivo* volumes of the SCM were calculated using the Cavalieri method. Modelling of the SCM was performed on five sets of computed tomography (CT) scans. This mapped the fascicular arrangement of the SCM with relation to the cervical motion segments, and used volume data from the MRIs to calculate realistic peak force capabilities.

Results

Dissection showed the SCM has four parts; sterno-mastoid, sterno-occipital, cleido-mastoid and cleido-occipital portions. Force modelling shows that peak torque capacity of the SCM is higher at lower cervical levels, and minimal at higher levels. Peak shear forces are higher in the lower cervical spine, while compression is consistent throughout.

Conclusions

The findings provide detailed insight into the structure and function of the SCM with relation to the cervical motion segments, and will help inform models of neck muscle function and dysfunction.

Introduction

The sternocleidomastoid (SCM) is a major muscle of the cervical spine, classically used to define the anterior and posterior triangles of the neck. Clinical interest in the role of the SCM [11] and its contribution to neck disorders [19] relies on a detailed understanding of neck muscle structure and function. This understanding is often based on information found in anatomical texts, with a supporting role from the research literature. Last [16] eloquently summarises how anatomical texts portray the SCM in three short sentences: "This muscle is usually not adequately described. The French anatomists describe it with great precision. It consists of four parts." (pg. 520). These statements remain relevant today.

Review of a selection of modern, commonly used anatomical texts revealed general agreement on the structure of the SCM, but limited detail of its fascicular arrangement. The SCM is typically described as arising from the manubrium and medial third of the clavicle inferiorly, and attached to the mastoid process and superior nuchal line superiorly [17, 24, 25]. However, the texts are vague regarding how the fibres of the SCM are arranged between these bony landmarks. Last [16] resolves this deficiency with a four-part description including sterno-mastoid (SM), sterno-occipital (SO), cleido-mastoid (CM) and cleido-occipital (CO) portions. These portions were previously described and clearly illustrated by Testut [27] in 1899, and reinforced more recently in the research literature [14].

Regarding function, modern anatomical texts generally agree that acting unilaterally the SCM produces ipsilateral lateral flexion and contralateral rotation of the head; bilateral contraction results in flexion of the neck with extension at the upper cervical levels, and when acting bilaterally on the thorax the muscle elevates the sternum and clavicle [17, 24, 25]. For general purposes such descriptions are entirely adequate, but lack detail for those interested in the magnitude or direction of the forces exerted by the muscle. With little attention paid to the four-part structure of the SCM not much is known about the force contributions of each portion.

An altered movement strategy of the neck involving increased SCM activity is purported to play a role in chronic neck pain [7], whiplash [12], and cervicogenic headache [4]. Common to these studies is a procedure described as the cranio-cervical flexion test, during which the SCM has been shown to have increased activity. Jull et al. [13] describe the cranio-cervical flexion test as a low-load nodding (upper cervical flexion) task performed in supine described as a test of the action of the deep cervical neck flexors (longus capitis and colli), and performed in a way so as to reduce excessive use of the SCM. This is based on the concept that the nodding action more specifically targets the anatomical action of the longus capitis and colli, and that SCM activity is either not required or undesirable [13, 20]. Yet beyond moments in the upper vs. lower cervical spine reported by Vasavada et al. [29], there is limited information available describing the forces that the SCM is capable of producing throughout the neck. The relationship between pain intensity and SCM activity is only modest, suggesting that other factors influence SCM activity in chronic neck pain [19]. In order to understand these factors, a more detailed understanding of the normal biomechanical capabilities of the SCM throughout the neck is required.

Vasavada et al. [29] examined how the morphology and moment arms of various neck muscles influenced their moment-generating capacity throughout the range of motion. Based on a model of simultaneous and maximal activation they provided estimates of the isometric moment generating capacity for flexion, lateral flexion and rotation in various positions. Cervical spine kinematics were simplified to two motion segments; upper and lower cervical. The moment-generating capacity for flexion was found to almost double in 40- 50° flexion due to an increased moment arm for the SCM, while potentially decreasing to less than 25% in extremely extended postures due to reduced moment arms. A strength of the data presented is that it supports and supplements textbook descriptions of the muscle actions, which concentrate on muscle actions in the neutral position. For the SCM in particular, limited information is available about the distribution of the forces across the individual motion segments, or the contributions of each portion of the SCM.

Force modelling derived from cadaveric muscle volumes is unlikely to accurately represent young, healthy individuals as cadaveric muscle volumes are often reduced in comparison [18, 26]. Modern imaging techniques provide an alternative data

source. In the research setting, muscle tissues are commonly imaged using ultrasound [22] and MRI [8, 10, 28]. Both methods are generally safe, allowing research to be undertaken on normal subjects with minimal risk or discomfort. MRI has some advantages, as images are more comprehensive and are less operator-dependent. Two studies have demonstrated that muscle volumes measured using MRI are significantly related to peak torque determined by dynamometry. Fukunaga et al [8] measured peak torque and muscle volumes in the elbow flexors and extensors, and Gadeberg et al [10] similarly examined the ankle dorsi and plantarflexors. Using MRI provides an excellent estimation of *in vivo* muscle volumes that complement the accuracy of dissection in detailing the structural arrangement of muscle fascicles.

The purpose of this research is to utilise both traditional dissection and modern imaging methods to provide detailed anatomical and biomechanical insight into the structure and functional capabilities of the SCM in the cervical spine. This will help inform models of neck muscle function and dysfunction.

Materials and Methods

This study was performed in three parts. Dissection revealed the attachment sites, lengths and volumes of the muscle portions, while magnetic resonance imaging (MRI) provided *in vivo* muscle volume data. The peak force generating capacities of the muscle portions were then modelled on computed tomography scans of the head and neck.

Dissection

Dissection was performed on six embalmed cadavers (three males age 73-74 years, three females age 63-93 years) with University ethical approval. In each cadaver the SCM was exposed, and divided into portions based on the attachment sites of each fascicle. Morphological data were recorded for each fascicle, including length and volume. Length was measured to the nearest millimetre using a metal ruler, both including tendinous tissue ('muscle length') and excluding tendinous tissue ('fascicle length'). Volume was measured to 0.1ml by water displacement in a measuring cylinder (according to Archimedes' principle). Where both sides of a cadaver were dissected the mean of morphological data gathered from both sides was calculated. The physiological cross-sectional area (PCSA) for each portion were calculated using the equation:

$$\text{PCSA} = \text{Fascicle volume} / \text{Fascicle length}$$

Magnetic Resonance Imaging

MRIs were performed on six young, healthy volunteers (three males age 24-37, three females age 26-28). Ethical approval was obtained from the Regional Ethics Committee (LRS/07/04/011). Each volunteer was scanned with a Philips Acheiva 1.X T machine using a neurovascular coil. Pilot scans were performed to optimise the image quality and minimise subject discomfort during the sequence. The sequence settings for the main images were three blocks of axial T1-weighted scans; each 32

slices, 3 mm thick with 0 mm gap, field of view 410mm, TR 500ms, TE 13ms, matrix 480 x 512, 4 'number of signals averaged' (NSA). For cross-reference purposes a single set of axial T2-weighted balanced fast field echo images were also taken; 96 slices, 3 mm thick with 0 mm gap, field of view 410mm, TR 5.2ms, TE 2.6ms, matrix 256 x 352, 2 NSA. The T1-weighted scan gave high quality images of the neck muscles, while the T2-weighted scan illustrated the vessels of the neck. The T2-weighted images ensured that vessels could be excluded from tracings of the muscle borders, for example the external jugular vein against the SCM.

Muscle volumes were calculated using the Cavalieri method, which is a well-established stereological method for calculating volumes from slices, that is both efficient and accurate [23]. This involved systematic sampling of slices from a random starting point. All parts of the muscle had an equal chance of being sampled, as the images were taken with no slice gap. This ensured our sample was unbiased. Our calculations were based on ~10 slices along the length of the muscle in line with recommendations of Roberts et al. [23]. Whole muscle cross-sectional muscle areas were traced in the sampled slices using OsiriX software (a freely available DICOM viewer), after which the volume of the muscle could be estimated. The accuracy of the area measurements was validated by performing area measurements on an object of known dimensions scanned in a weekly quality assurance test, then analysing the differences with paired t-tests. Reproducibility was checked by repeating the measurements in one of the subjects (randomly selected), and performing an intra-class correlation (ICC).

Biomechanical Modelling

Modelling of the SCM was performed on five sets of computed tomography (CT) scans from oncology archives in a tertiary-level public hospital (four males mean age 50 years, one female 57 years). Further ethical approval was obtained from the Regional Ethics Committee for this part of the study (LRS/06/09/037). This was performed using OsiriX software, and involved plotting three-dimensional coordinates for the attachment points of each portion of the SCM, instantaneous axes of rotation (IARs), and vertebral body tilt angles relative to the (arbitrary) neutral

position in the sagittal plane. These coordinates and angles could then be used to calculate the torque, compression and shear force generated by each muscle portion across the cervical motion segments. Calculations were based on morphological data from the earlier dissection and MRI components of this research.

The attachment points of each portion of the SCM were based on those identified in the dissection study. The positions of the IARs are important for torque calculations, and were plotted from C2/3 to C6/7 based on the previous work of Amevo et al. [1-3]. In these studies the authors showed that the IAR of each motion segment is found within the outline of the lower vertebra, and normalized this coordinate system so that the position of the IAR within the vertebral body outline can be expressed as a proportion of the vertebral height and width. Positions of the IARs for the atlanto-occipital and atlanto-axial joints were not available. The vertebral tilt angle in the sagittal plane refers to the degree to which each vertebra is tilted anteriorly (or posteriorly) from the transverse plane, which is an important consideration when calculating shear and compression forces.

To incorporate the muscle volumes obtained from healthy young volunteers in the MRI study, the PCSA values from dissection study needed to be recalculated, this time substituting MRI muscle volumes into the equation (PCSA = Fascicle volume / fascicle length). Because the MRI study generated whole SCM muscle volumes, in order to model the forces generated by each portion of the SCM the whole muscle volumes needed to be divided into portions. This was done by calculating the percentage contribution of each portion to total muscle volume in the dissection data, and then dividing the SCM muscle volume from MRI into the same proportions. This provided an estimate of the *in vivo* portion volumes in males and females. Fascicular length values were taken from the dissection study of cadaveric material, as there was no reliable way of determining fascicle length (excluding tendinous tissue) *in vivo* from the MR images. These fascicle lengths, along with the calculated fascicular volumes enabled the PCSA of each portion to be estimated for young, healthy males and females. These data were then entered into the biomechanical modeling spreadsheets to produce force estimates.

Calculations

Force estimates were calculated based on the equation:

$$\text{Peak force} = \text{PCSA} \times \text{Specific tension (K)}$$

Note that the specific tension is a constant that reflects the relationship between muscle PCSA and peak force, and has been calculated by several researchers. Results vary, so in line with previous work a value of specific tension (K) has not been entered [5]. Force estimates are presented as an expression of specific tension, allowing readers to recalculate the forces using their preferred value of specific tension if desired.

Shear and compression

Anterior – posterior shear and vertical compression were derived from the orientation of the fascicle in the sagittal plane. Shear and compression represent the two perpendicular vector components of the sagittal force produced by each fascicle. Each value was calculated with reference to the vertebral tilt angle of a particular vertebral level to account for changes in the vertebral tilt through the cervical spine. This involved calculating the sagittal (y and z) components of the force produced by each fascicle with reference to the vertebral tilt of each vertebral level, as described and illustrated by Bogduk et al. [5].

A fascicle's unit direction vector was computed by taking the difference of the x, y and z coordinates at each of its attachment sites, and then dividing by the length of the fascicle (obtained by the Pythagorean Theorem). The orientation of the shear and compression forces was obtained using the measured angle of vertebral tilt to establish a frame of reference. The magnitude of these forces was then computed by projecting the muscle unit vector, multiplied by the peak force values in each of these directions. The specific tension (K) was not included at this point in the calculation, so the peak force was represented by the PCSA value.

Torque

Torque was calculated as the force capacity in the sagittal plane (muscle vector) multiplied by the length of the moment vector (MV). The moment vector is simply the line from the IAR of the vertebrae to the fascicle, which meets it at right angles (Fig. 1). The force capacity in the sagittal plane is obtained by multiplying the peak force of the muscle (using the PCSA value again in the absence of a specific tension) by the length of its projection to the sagittal plane divided by its total length.

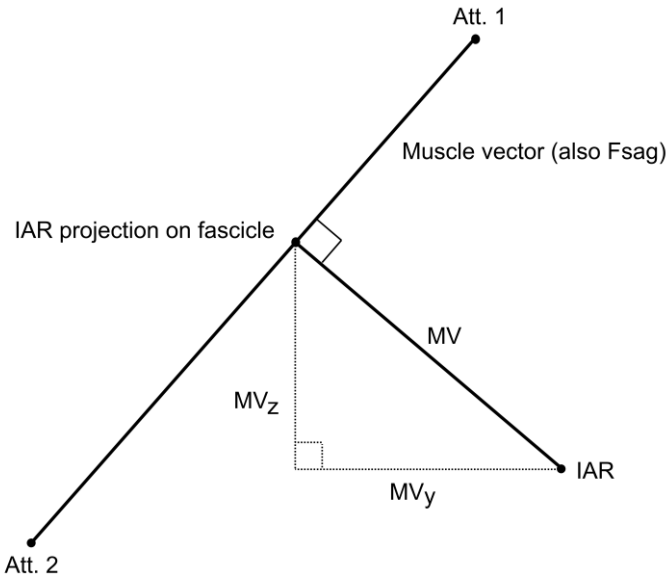

Fig 1. Diagrammatic representation of the components used in the torque calculation. Att. 1 and Att. 2 are the attachment sites of the fascicle, IAR is the instantaneous axis of rotation, MV is the moment vector, and the IAR projection on muscle is the point at which the muscle and moment vectors meet at a right angle. MVz and MVy represent the component vectors of MV.

Results

Dissection

Dissection revealed that the SCM was formed of four portions (sterno-mastoid, sterno-occipital, cleido-mastoid and cleido-occipital portions) based on attachment sites (Fig. 2). The two clavicular portions were distinctly separate superiorly, with the sternal portions interposed between them. The two sternal portions were not morphologically distinct, but rather divided for modelling purposes at the junction of the mastoid process and the superior nuchal line. In terms of volume and PCSA the sterno-mastoid portion was largest, followed by the approximately equal cleido-mastoid and sterno-occipital portions. The cleido-occipital portion was the smallest (Table 1). Male muscle volumes were significantly larger than those in females ($p < 0.05$) (Table 2).

Table 1. Morphological data from dissection (standard deviation)

	Portion	**n**	**Mean muscle length in cm**	**Mean fascicle length in cm**	**Mean volume in ml**	**Mean PCSA in cm^2**
Males	SM	3	20.9 (0.9)	14.1 (1.1)	10.1 (0.8)	0.7 (0.1)
	SO	3	22.9 (0.5)	15.1 (1.2)	5.7 (0.7)	0.4 (0.1)
	CM	3	16.2 (1.2)	11.9 (0.7)	5.6 (1.0)	0.5 (0.1)
	CO	3	19.6 (1.2)	15.2 (0.9)	3.5 (2.0)	0.2 (0.1)
	Overall	**3**	**19.9 (0.7)**	**14.1 (0.8)**	**24.8 (3.9)**	**1.8 (0.3)**
Females	SM	3	18.8 (0.8)	13.6 (2.5)	7.1 (2.4)	0.5 (0.1)
	SO	3	21.2 (2.2)	12.7 (1.7)	3.2 (1.3)	0.3 (0.1)
	CM	3	13.9 (1.9)	10.0 (1.9)	3.7 (1.8)	0.5 (0.2)
	CO	3	19.0 (2.1)	12.7 (2.6)	1.2 (0.7)	0.1 (0.0)
	Overall	**3**	**18.2 (1.6)**	**12.3 (1.6)**	**15.2 (4.8)**	**1.3 (0.3)**

SM = Sterno-mastoid, SO = Sterno-occipital, CM = Cleido-mastoid, CO = Cleido-occipital

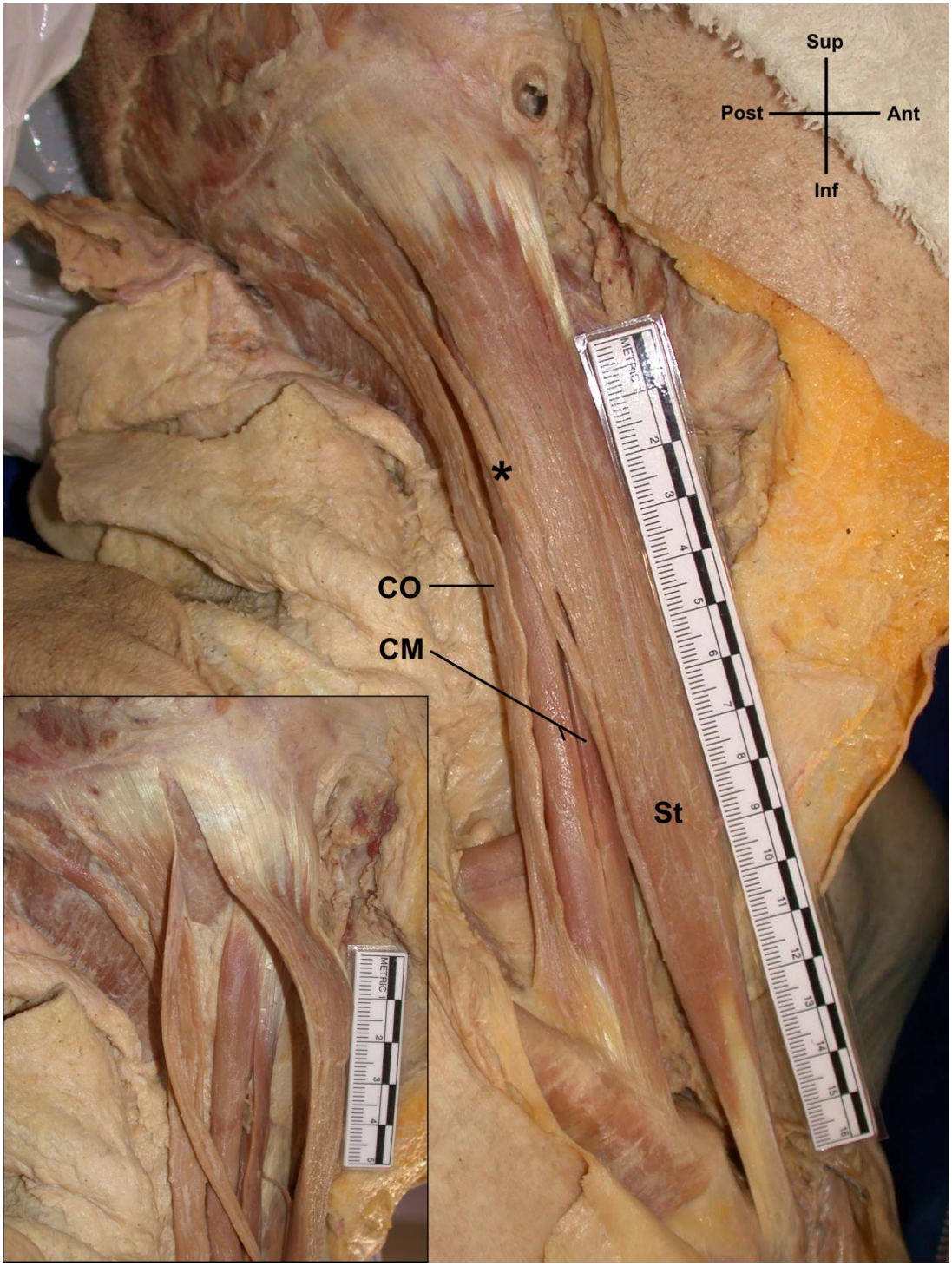

Fig 2. Lateral view of a dissection of the right sternocleidomastoid. Note the visibly separate sternal (St), cleido-mastoid (CM) and cleido-occipital (CO) portions. The sterno-mastoid and sterno-occipital portions are not distinct, but superiorly attach to the mastoid process and superior nuchal line respectively. * indicates a visibly distinct portion of the sterno-occipital portion present in this dissection. Inset: Retracting the sternal portions superiorly reveals the deep cleido-mastoid portion.

Magnetic resonance imaging

Review of the area measurement accuracy showed a mean difference of 0.04 cm^2 with 95% limits of agreement from -0.10 to 0.19 cm^2 between the measured area and the true value (represented by a scanned object of known dimensions). This tells us that on average the measurement method under-estimates the true value by approximately 0.04 cm^2 (this is sometimes referred to as the bias), which was considered acceptable. For the re-measured muscle volumes the ICC was 0.993 with a 95% confidence interval of 0.951 – 0.999.

The MR images revealed significantly larger muscle volumes when compared to dissection data (Table 2). As for the dissection data, a significant difference between male and female muscle volumes was noted in the MRI data.

Table 2. Comparison of mean muscle volumes from dissection and MRI (standard deviation).

	Dissection volumes in cm^3	**MRI volumes in cm^3**	**P-value**
Males (n=3)	24.8 (3.9)	72.0 (8.0)	<0.01
Females (n=3)	15.2 (4.8)	39.4 (12.0)	0.03
P-value	0.03	0.01	

Biomechanical Modelling

The force generating capabilities of the SCM per portion and cervical level are shown in Tables 3-5. As noted earlier values are presented as an expression of specific tension (K), so most readily allow comparisons between the portions of the SCM. To obtain an absolute force estimate the presented values need to be multiplied by a specific tension value. To see absolute estimates of peak force generating capabilities (using a specific tension of 15 N/cm^2) refer to Appendix A. The male and female data showed a similar distribution of forces, but consistently lower force estimates seen in females. The sagittal orientation of the forces based on muscle attachment sites and their relation to the IARs are shown in Figure 3.

The relationship between the individual portions of the SCM and the IARs determined if the portion was capable of exerting a flexion or extension force. The level(s) at

which this muscle crossed the IARs of the cervical spine was highly dependent on head and neck position of the models, which is reflected in relatively high standard deviations. At C6/7 a net flexion moment was found, while at higher cervical levels this moment reduced, until finally at C2/3 the net result was an extension moment. At C2/3 the occipital portions typically crossed posterior to the IARs, and the mastoid portions anteriorly (Fig. 3). Compression generating capability was greatest in the upper cervical spine, and reduced with descending levels. Shear generating capability was especially low in the upper cervical levels, reflecting the slight posterior vertebral tilt of these levels, and increased gradually until compression and shear were relatively equal at the level of C7/T1. The larger sterno-mastoid portion accounted for the greatest part of the force estimate, especially compression given its more vertical orientation. The small cleido-occipital portion accounted for the smallest contribution, even in shear force despite its oblique orientation.

To give readers a sense of absolute peak force estimates, the results with a specific tension value of 15 N/cm^2 are presented in Appendix A.

Table 3. Mean peak flexion torque (standard deviation) exerted by the SCM as an expression of specific tension (K)

		C2/3	C3/4	C4/5	C5/6	C6/7
Males	SM	0.01K (0.03)	0.03K (0.02)	0.04K (0.02)	0.06K (0.02)	0.07K (0.03)
	SO	-0.01K (0.02)	0.00K (0.02)	0.01K (0.01)	0.02K (0.01)	0.03K (0.01)
	CM	0.01K (0.01)	0.02K (0.01)	0.03K (0.01)	0.04K (0.01)	0.04K (0.02)
	CO	-0.02K (0.01)	-0.01K (0.01)	0.00K (0.01)	0.00K (0.01)	0.01K (0.01)
	Total	**-0.01K (0.02)**	**0.04K (0.02)**	**0.08K (0.02)**	**0.12K (0.02)**	**0.15K (0.03)**
Females	SM	0.01K (0.02)	0.02K (0.01)	0.03K (0.01)	0.04K (0.01)	0.05K (0.02)
	SO	-0.01K (0.01)	0.00K (0.01)	0.01K (0.01)	0.01K (0.01)	0.02K (0.01)
	CM	0.01K (0.01)	0.01K (0.01)	0.02K (0.01)	0.03K (0.01)	0.03K (0.01)
	CO	-0.01K (0.00)	0.00K (0.00)	0.00K (0.00)	0.00K (0.00)	0.00K (0.00)
	Total	**0.00K (0.01)**	**0.03K (0.01)**	**0.05K (0.01)**	**0.08K (0.02)**	**0.10K (0.02)**

Minus (-) signs indicate an extension force. SM = Sterno-mastoid, SO = Sterno-occipital, CM = Cleido-mastoid, CO = Cleido-occipital. C2/3 = Vertebral level of C2 on C3, C3/4 = Vertebral level of C3 on C4, etc.

Table 4. Mean anterior shear forces (standard deviation) exerted by the SCM as an expression of specific tension (K)

		C0/1	C1/2	C2/3	C3/4	C4/5	C5/6	C6/7	C7/T1
Males	SM	0.30 (0.52)	0.28 (0.35)	1.00 (0.14)	1.00 (0.12)	1.09 (0.08)	1.22 (0.180	1.35 (0.21)	1.45 (0.21)
	SO	0.26 (0.25)	0.25 (0.17)	0.62 (0.08)	0.62 (0.06)	0.67 (0.06)	0.73 (0.10)	0.79 (0.11)	0.84 (0.11)
	CM	0.08 (0.37)	0.06 (0.25)	0.55 (0.10)	0.55 (0.10)	0.62 (0.03)	0.71 (0.09)	0.80 (0.12)	0.88 (0.13)
	CO	0.22 (0.13)	0.21 (0.10)	0.43 (0.05)	0.43 (0.04)	0.46 (0.03)	0.49 (0.05)	0.52 (0.06)	0.55 (0.06)
	Total	**0.86 (0.33)**	**0.80 (0.24)**	**2.60 (0.24)**	**2.60 (0.23)**	**2.84 (0.25)**	**3.14 (0.29)**	**3.47 (0.33)**	**3.72 (0.36)**
Females	SM	0.20 (0.34)	0.18 (0.23)	0.65 (0.09)	0.65 (0.08)	0.71 (0.05)	0.79 (0.12)	0.88 (0.14)	0.94 (0.14)
	SO	0.16 (0.15)	0.15 (0.10)	0.37 (0.05)	0.37 (0.04)	0.40 (0.03)	0.43 (0.06)	0.47 (0.07)	0.50 (0.07)
	CM	0.05 (0.27)	0.04 (0.18)	0.39 (0.07)	0.39 (0.07)	0.44 (0.02)	0.50 (0.07)	0.57 (0.08)	0.63 (0.09)
	CO	0.08 (0.05)	0.08 (0.04)	0.16 (0.02)	0.16 (0.02)	0.17 (0.01)	0.18 (0.02)	0.20 (0.02)	0.21 (0.02)
	Total	**0.49 (0.22)**	**0.45 (0.15)**	**1.57 (0.20)**	**1.57 (0.18)**	**1.72 (0.21)**	**1.91 (0.23)**	**2.11 (0.28)**	**2.27 (0.28)**

SM = Sterno-mastoid, SO = Sterno-occipital, CM = Cleido-mastoid, CO = Cleido-occipital. C0/1 = Vertebral level of Occiput on C1, C1/2 = Vertebral level of C1 on C2, etc.

Table 5. Mean compression forces (standard deviation) exerted by the SCM as an expression of specific tension (K)

		C0/1	C1/2	C2/3	C3/4	C4/5	C5/6	C6/7	C7/T1
Males	SM	1.92K (0.16)	1.96K (0.10)	1.73K (0.10)	1.73K (0.09)	1.68K (0.05)	1.58K (0.12)	1.46K (0.18)	1.36K (0.19)
	SO	1.01K (0.10)	1.03K (0.06)	0.87K (0.06)	0.87K (0.04)	0.84K (0.04)	0.78K (0.10)	0.71K (0.13)	0.65K (0.14)
	CM	1.30K (0.07)	1.33K (0.04)	1.23K (0.05)	1.23K (0.05)	1.20K (0.02)	1.14K (0.05)	1.07K (0.08)	1.01K (0.10)
	CO	0.60K (0.07)	0.61K (0.04)	0.50K (0.04)	0.50K (0.03)	0.47K (0.03)	0.43K (0.07)	0.39K (0.09)	0.35K (0.10)
	Total	**4.84K (0.50)**	**4.93K (0.51)**	**4.33K (0.47)**	**4.33K (0.47)**	**4.19K (0.46)**	**3.94K (0.45)**	**3.63K (0.43)**	**3.37K (0.41)**
Females	SM	1.25K (0.11)	1.27K (0.07)	1.12K (0.06)	1.13K (0.06)	1.09K (0.03)	1.03K (0.08)	0.95K (0.12)	0.88K (0.13)
	SO	0.60K (0.06)	0.61K (0.04)	0.52K (0.03)	0.52K (0.03)	0.50K (0.02)	0.46K (0.06)	0.42K (0.08)	0.38K (0.08)
	CM	0.93K (0.05)	0.95K (0.03)	0.87K (0.04)	0.87K (0.04)	0.85K (0.01)	0.82K (0.04)	0.77K (0.06)	0.72K (0.07)
	CO	0.23K (0.02)	0.23K (0.02)	0.19K (0.01)	0.19K (0.01)	0.18K (0.01)	0.16K (0.03)	0.15K (0.03)	0.13K (0.04)
	Total	**3.00K (0.39)**	**3.06K (0.40)**	**2.70K (0.37)**	**2.70K (0.37)**	**2.62K (0.36)**	**2.47K (0.34)**	**2.28K (0.33)**	**2.12K (0.31)**

SM = Sterno-mastoid, SO = Sterno-occipital, CM = Cleido-mastoid, CO = Cleido-occipital. C0/1 = Vertebral level of Occiput on C1, C1/2 = Vertebral level of C1 on C2, etc.

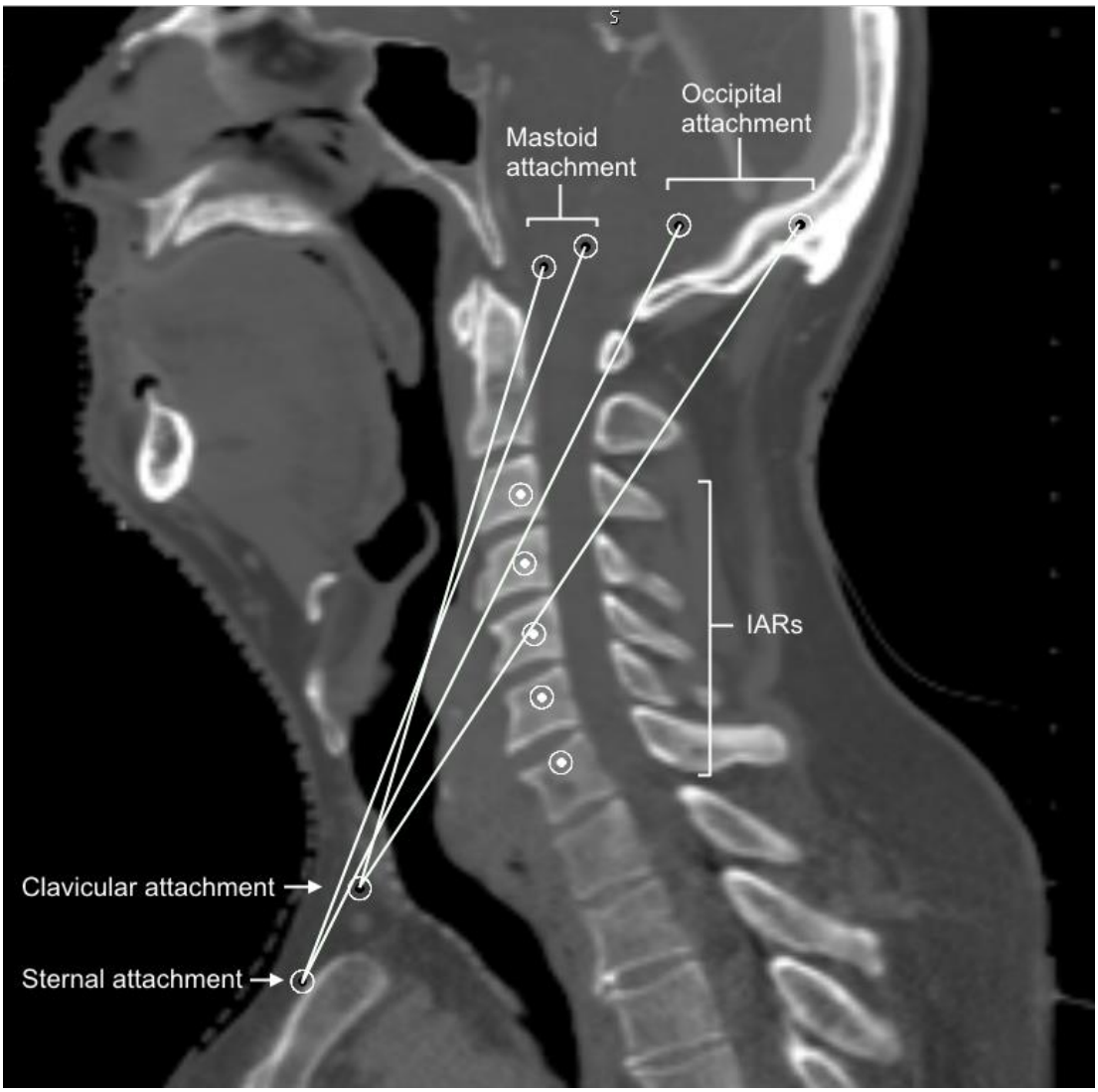

Fig 3. A CT image illustrating the location of the instantaneous axes of rotation (IARs) in relation to the SCM attachment sites and orientation.

Discussion

The purpose of this study was to describe the detailed anatomy of the SCM, and estimate its force capabilities and distribution across the cervical motion segments. This study combined aspects of traditional anatomical dissection with modern imaging to present a novel methodology. The findings show that the SCM has four parts, consistent with previous literature [14, 27], but not typically described in modern anatomical texts. Biomechanical modeling revealed clear differences in the forces exerted across the motion segments.

The methods outlined in this research incorporate traditional methods of dissection with modern imaging to obtain *in vivo* muscle volumes (via MRI) and model three-dimensional peak force capabilities (via CT). Dissection remains the only way of accurately determining the fascicular arrangement and morphology of a muscle, but a common criticism is that dissection volumes in elderly cadavers do not reflect living tissue. This criticism was addressed in this study by combining dissection with MRI volumes. A limitation of this approach is that while whole muscle volumes could be accurately measured using MRI, individual muscle portion volumes could not. Calculating the portion volumes based on the proportions found in dissection was necessary in order to calculate force estimates for each muscle portion. While it would have been better if the muscle portions could have been visualised on MRI, this method certainly more accurately represents *in vivo* muscle volumes. This study promotes the use of the Cavalieri method to calculate muscle volumes from MRI slices. As has been previously reported, this method is efficient, unbiased and accurate [23], and well suited to muscle volume calculations [10].

This study demonstrates substantial differences between cadaveric and MRI muscle volumes (Table 2). Muscle volume seems to be the variable most affected by both age [18] and embalming [26], while also being a major determinant of joint torque [10]. Other variables, while important, have a less critical impact on estimates of peak torque [8]. For these reasons it is important to achieve the most realistic estimate of muscle volume possible in force modeling studies. This further supports the use of *in vivo* MRI muscle volumes to model peak force capabilities.

Previous similar modelling of peak force generating capacities of muscles affecting the spine has used radiographs to determine the bony landmarks necessary for the lumbar back muscles [5]. For this study radiographs were considered inappropriate, as parts of the upper cervical spine and C7 are typically obscured. Computed tomography (CT) scans allow the same basic methodology without needing to digitise points manually. Compared to MRI, CT images give clearer three-dimensional images of the bony landmarks, and are more spatially accurate [15]. The main drawback is that CT scans are performed in the supine position rather than upright. This was considered to be a fair approximation of the upright position in the context of this study given that other imaging options had more substantial drawbacks.

The four-part structure of the SCM was consistent in all the dissections, and with previous literature. This suggests that the small number of dissections were sufficient to describe the fascicular arrangement of the muscle. Modern anatomical texts certainly document the attachment sites accurately, but often lack detail of the muscle arrangement. The mastoid portions had greater PCSAs, approximately double that of the occipital portions. As a result force generated by the SCM will be directed more greatly through the mastoid process. The more angulated cleido-occipital portion is relatively smaller, reducing the ability of the SCM to produce more oblique forces. A practical implication is that forces resulting from the oblique orientation of the SCM (such as extension at higher levels) may be lower than expected. The effect of these size and orientation differences on the force capabilities are shown in Table 3.

Biomechanical modeling also revealed clear differences in the forces the SCM could exert on the upper and lower cervical spine (Tables 3-5). The peak torque generating capacity of the SCM at C2/3 was negligible. In the absence of precise documented IARs for the atlanto-occipital and atlanto-axial joints peak torque estimates were not calculated. However, one could infer that at least in the neutral position the torque generating capacity of the SCM is likely to remain small at upper levels. As noted earlier, the larger mastoid portions have more vertical trajectory (see Fig. 3) and would contribute to extension less than the smaller occipital portions at higher levels. In the upper cervical spine the primary force capability was for compression. The shear generating capacity was minimal in the upper cervical spine, especially from the

occiput to C2. This increased in the lower cervical spine to approximately equal compression. As can be inferred from Fig. 3, the facet orientation (oblique postero-inferiorly) in the lower cervical spine is almost perpendicular to the alignment of the SCM. As a result, contraction of the SCM will certainly result in compression of the facet joints in addition to the compression (of the vertebral body) shown in the calculations. Thus, the facet joints will oppose shear forces generated by the SCM at lower cervical levels, effectively stabilizing the cervical spine. As argued by Penning [21] the axis of rotation is predominantly determined by the orientation of the zygapophysial joints. The IARs are located further inferior for C2/3 than for C6/7 [2], resulting in a more 'gliding' pattern of motion at C2/3 compared to more 'tilting' at C6/7 [21]. This highlights that although the SCM may be capable of generating shear at lower cervical levels, *in vivo* many structures (particularly the zygapophysial joints) will counteract and functionally modify this force.

The values for peak torque are relatively small (Table 3), which is perhaps surprising considering the SCM is the largest muscle of the anterior neck. To discuss the size of the force values requires a value for the specific tension (K) coefficient, which is a source of debate. For a more complete view Fukunaga et al. [9] discusses the factors involved in detail. Muscle volume is arguably the most important factor in determining force calculations [8], and the way in which muscle volume is measured directly affects the value of specific tension. For studies measuring *in vivo* muscle volumes (as opposed to cadaveric volumes) using ultrasound or MRI specific tension values range between 8-24N/cm^2 [9]. For the purposes of discussion here 15 N/cm^2 represents a mid-range value. Using a specific tension value of 15 N/cm^2 results in a bilateral peak flexion capacity of 4.6 Nm at C6/7, and 0.1 Nm at C2/3 (see Appendix A). These estimates are broadly comparable to previous research by Vasavada et al. [29]. In this study the authors report a total flexion moment generating capacity of 4 Nm produced mainly by the SCM (69%), but with contributions from longus capitis and colli (17% total) and scalenus anterior (14%). However, because the authors do not report values with reference to specific cervical motion segments direct comparisons are not possible. To put these force values in context, the weight of the head (approx. 5 kg) with a one-centimeter moment arm would result in a moment of ~0.5 Nm. Given that functional movement should rarely require peak muscle activity the SCM seems capable of providing meaningful torque only in the lower cervical

spine.

This study may help researchers understand the biomechanical implications of SCM activity, and how this could contribute to neck disorders. A relative increase in SCM activity during the cranio-cervical flexion test has been shown in a range of cervical disorders (along with a decrease in activity of longus capitis and colli) [4, 6, 12, 19], yet it is not clear what biomechanical effect this activity generates. The biomechanical rationale described for utilizing the cranio-cervical flexion as a test and an exercise is that the deeper muscles provide cervical spine stability or control, while the larger more superficial muscles (SCM and scalenus anterior in particular) are movement generators that have a destabilizing effect [7]. The detailed biomechanical work of Winters and Peles [30] is typically cited in support of this rationale. Unfortunately, this rather oversimplifies an in-depth body of work. Winters and Peles [30] make this clear in the final point of their summary; "…xiii). perhaps the most fundamental conclusion of our study is that the internal paraspinal musculature is very important during voluntary movements; in fact, the large, multilink superficial muscles with larger moments arms may be more effective "stabilizers"." (pg. 477). At higher cervical levels this research shows the SCM is primarily capable of producing compression, and very limited torque. In light of the above statements, this compression could be considered a stabilizing role. At lower cervical levels is capable of generating greater flexion torque, along with anterior shear and further compression. As noted earlier, any anterior shear will be opposed by, and compress the zygapophysial joints – another mechanism by which the SCM could potentially act in a stabilizing role. It may be that patients with cervical disorders derive benefit from the stability that SCM activity potentially provides, and any clinical benefits associated with reduced SCM activity are due to lower compression forces across the vertebral bodies, intervertebral discs and zygapophysial joints.

This study has a number of limitations. In addition to the methodological limitations discussed, it should be recognized that the peak force generating capacities of the SCM portions remain an estimate. Other factors such as fibre type affect force production, but have not been considered in this model. Rather, this study design has sought to address the most important factors, in particular the fascicular arrangement of the SCM and *in vivo* muscle volumes for young healthy volunteers. Further, this

study addresses only the neutral position, and forces in the sagittal plane. How the force capacity of neck muscles changes with head and neck position has been described elsewhere [29]. While other planes could be examined with this methodology, the focus has been on sagittal plane forces as this is where previous research has established IAR positions, and where there is clinical relevance to the role of the SCM.

Conclusions

The SCM has a four-part structure based on attachment sites, and creates unique forces across the cervical motion segments. This study presents estimates of the muscle's peak force generating capacity based on realistic architecture and *in vivo* muscle volumes. The methods described are novel, bringing together traditional dissection and modern imaging to strengthen the overall methodology. The force generating capacity of the SCM is described per portion and across the cervical motion segments, contributing to our understanding of the role this muscle plays in neck muscle function and dysfunction.

Acknowledgement: The authors wish to acknowledge the contribution of Dr Susan Mercer to this project. She was deeply involved in the early stages of this research, and was a great mentor for the lead author. We also express our thanks to the individuals and families who generously bequeath their bodies for teaching and research, which make this work possible.

Funding: This research was funded at a departmental level, and received no external funding.

Conflict of interest: The authors declare that they have no conflicts of interest.

Ethical approval: All procedures performed involving human participants were in accordance with the ethical standards of the institutional and regional research committees and with the 1964 Helsinki declaration and its later amendments or comparable ethical standards.

List of figures

List of tables

Appendix A

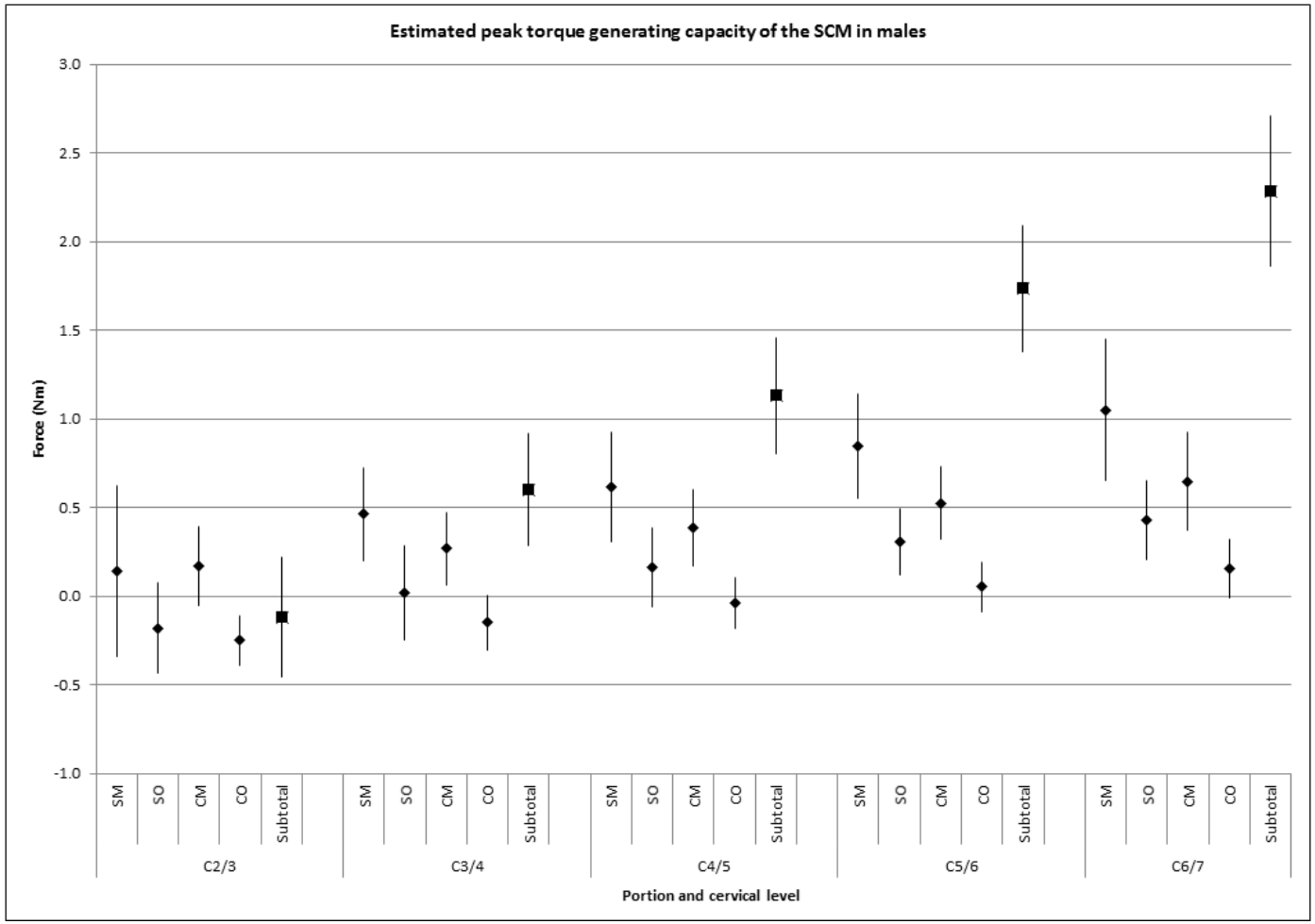
Estimated peak torque generating capacity of the SCM in males
Force (Nm)
3.0
2.5
2.0
1.5
1.0
0.5
0.0
-0.5
-1.0
SM
SO
CM
CO
Subtotal
C2/3
C3/4
C4/5
C5/6
C6/7
Portion and cervical level

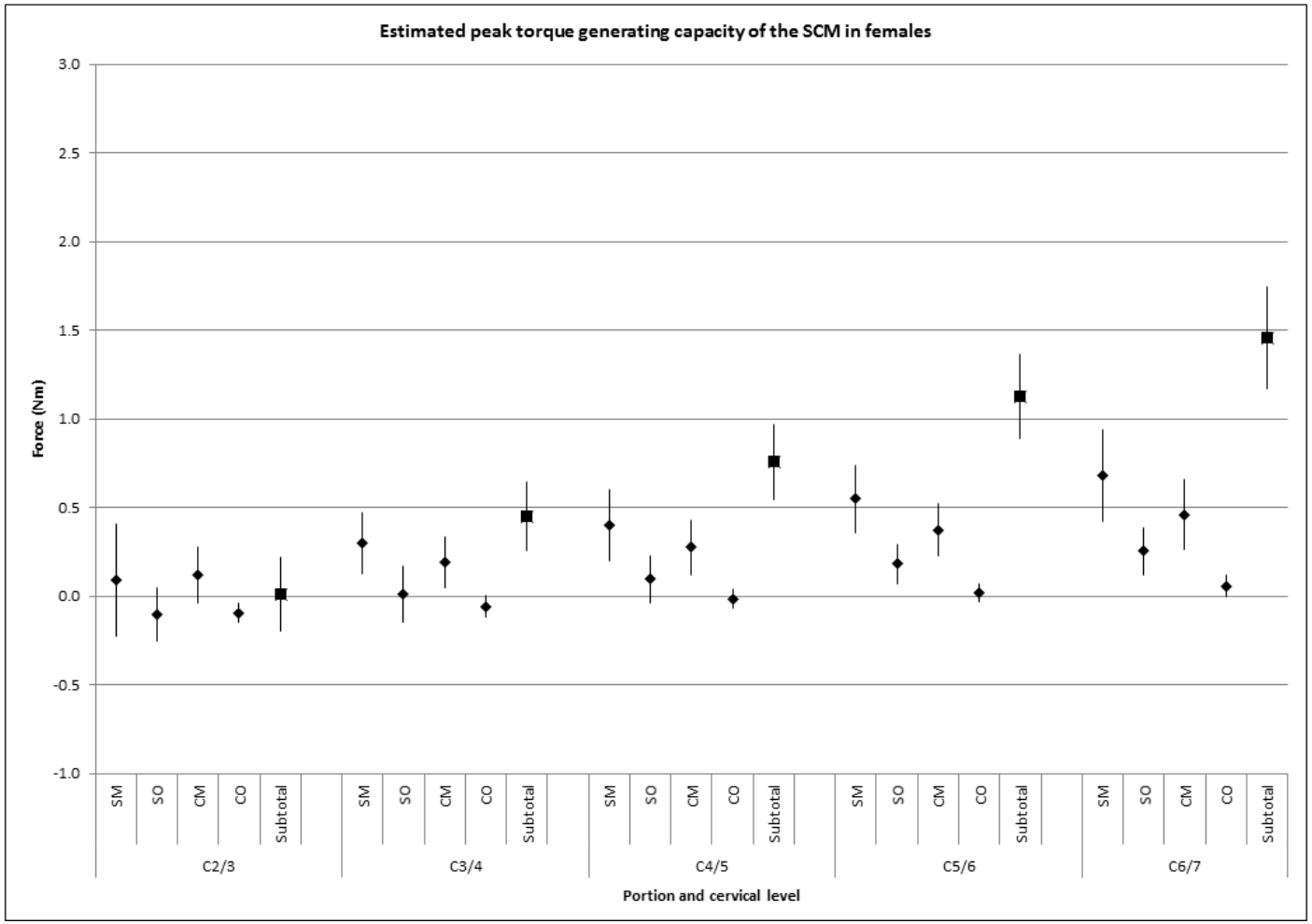
Estimated peak torque generating capacity of the SCM in females
Force (Nm)
3.0
2.5
2.0
1.5
1.0
0.5
0.0
-0.5
-1.0
SM
SO
CM
CO
Subtotal
C2/3
C3/4
C4/5
C5/6
C6/7
Portion and cervical level

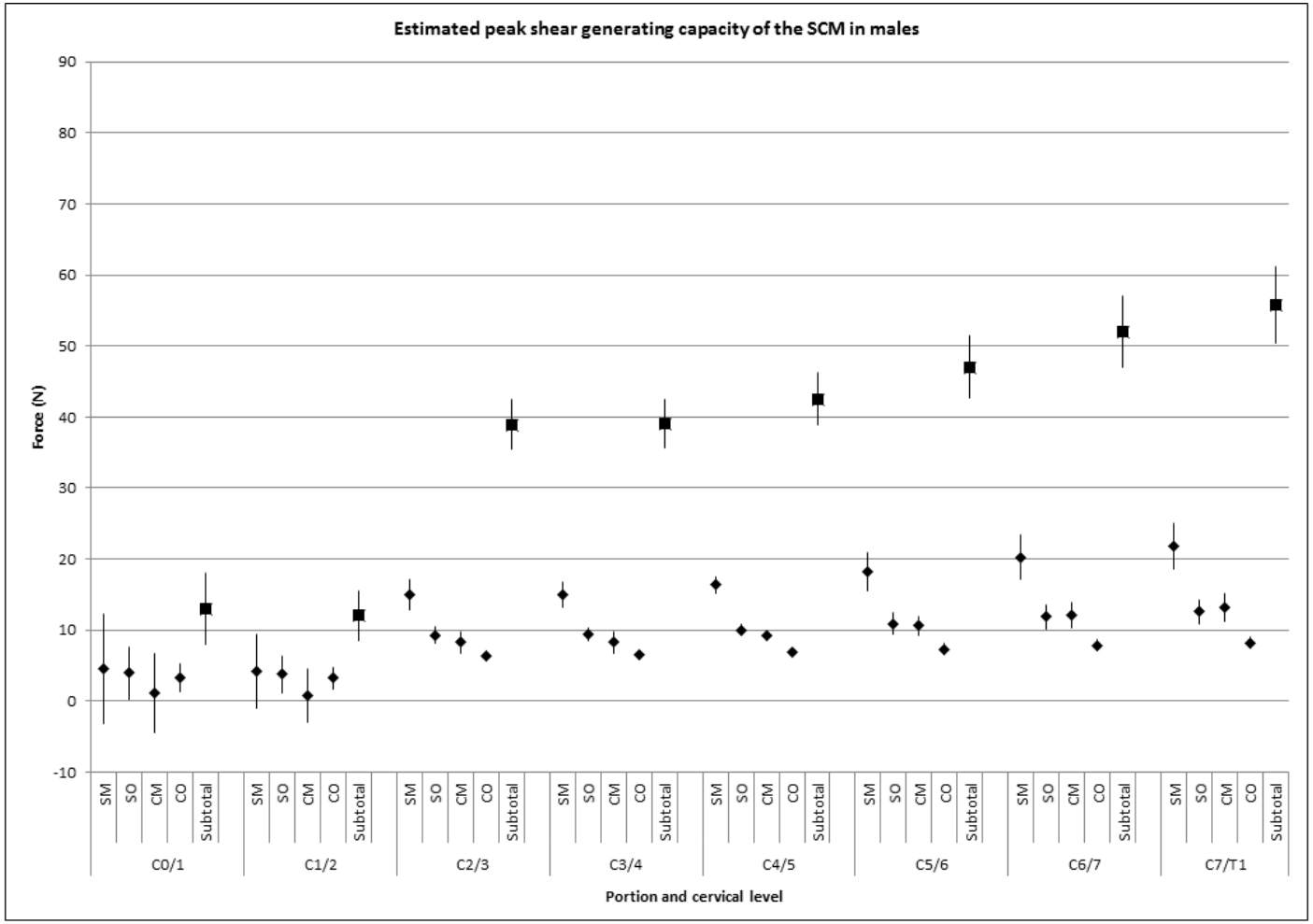
Estimated peak shear generating capacity of the SCM in males
Force (N)
90
80
70
60
50
40
30
20
10
0
-10
SM
SO
CM
CO
Subtotal
C0/1
C1/2
C2/3
C3/4
C4/5
C5/6
C6/7
C7/T1
Portion and cervical level

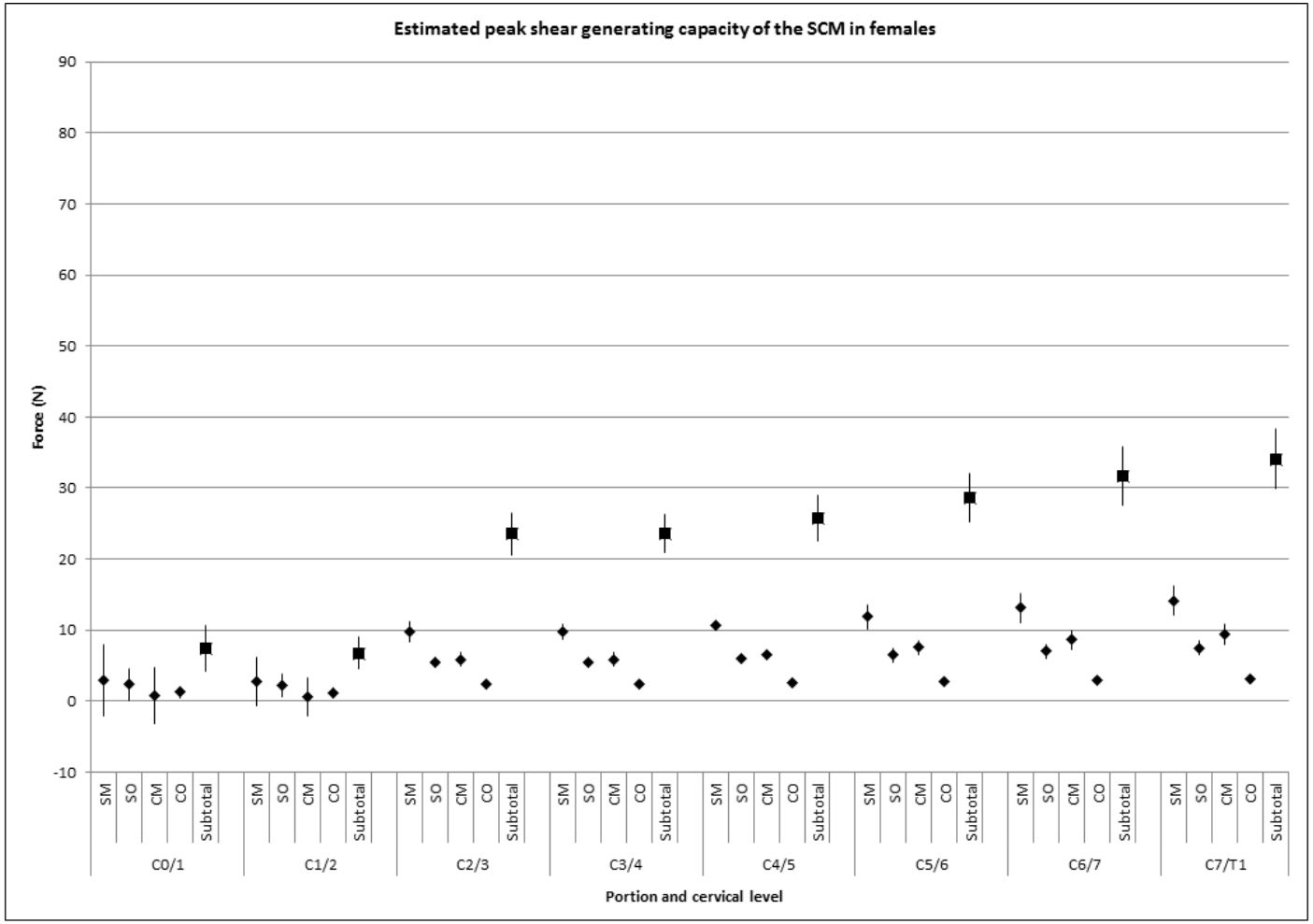
Estimated peak shear generating capacity of the SCM in females
Force (N)
90
80
70
60
50
40
30
20
10
0
-10
SM
SO
CM
CO
Subtotal
C0/1
C1/2
C2/3
C3/4
C4/5
C5/6
C6/7
C7/T1
Portion and cervical level

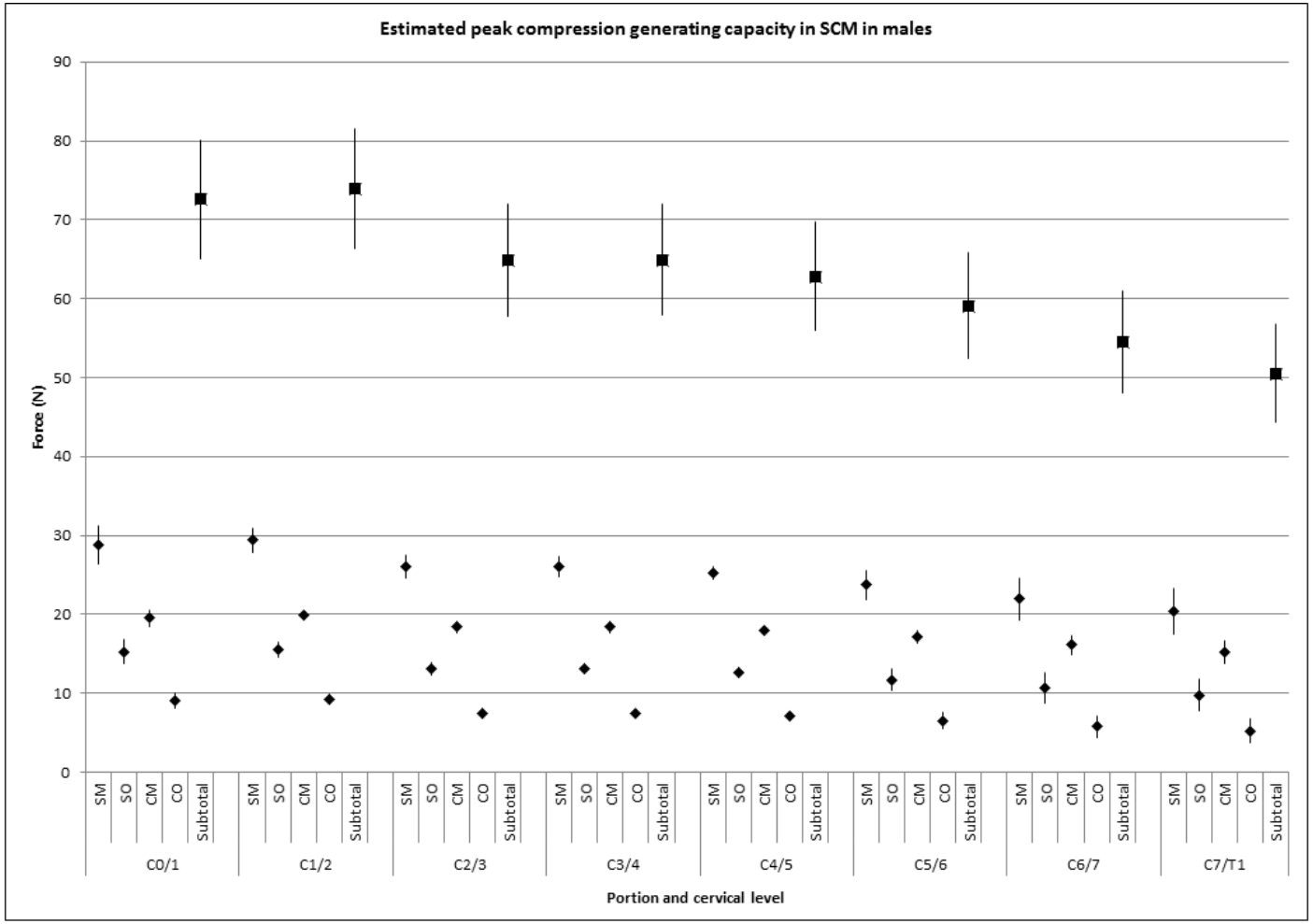
Estimated peak compression generating capacity in SCM in males
Force (N)
90
80
70
60
50
40
30
20
10
0
SM
SO
CM
CO
Subtotal
C0/1
C1/2
C2/3
C3/4
C4/5
C5/6
C6/7
C7/T1
Portion and cervical level

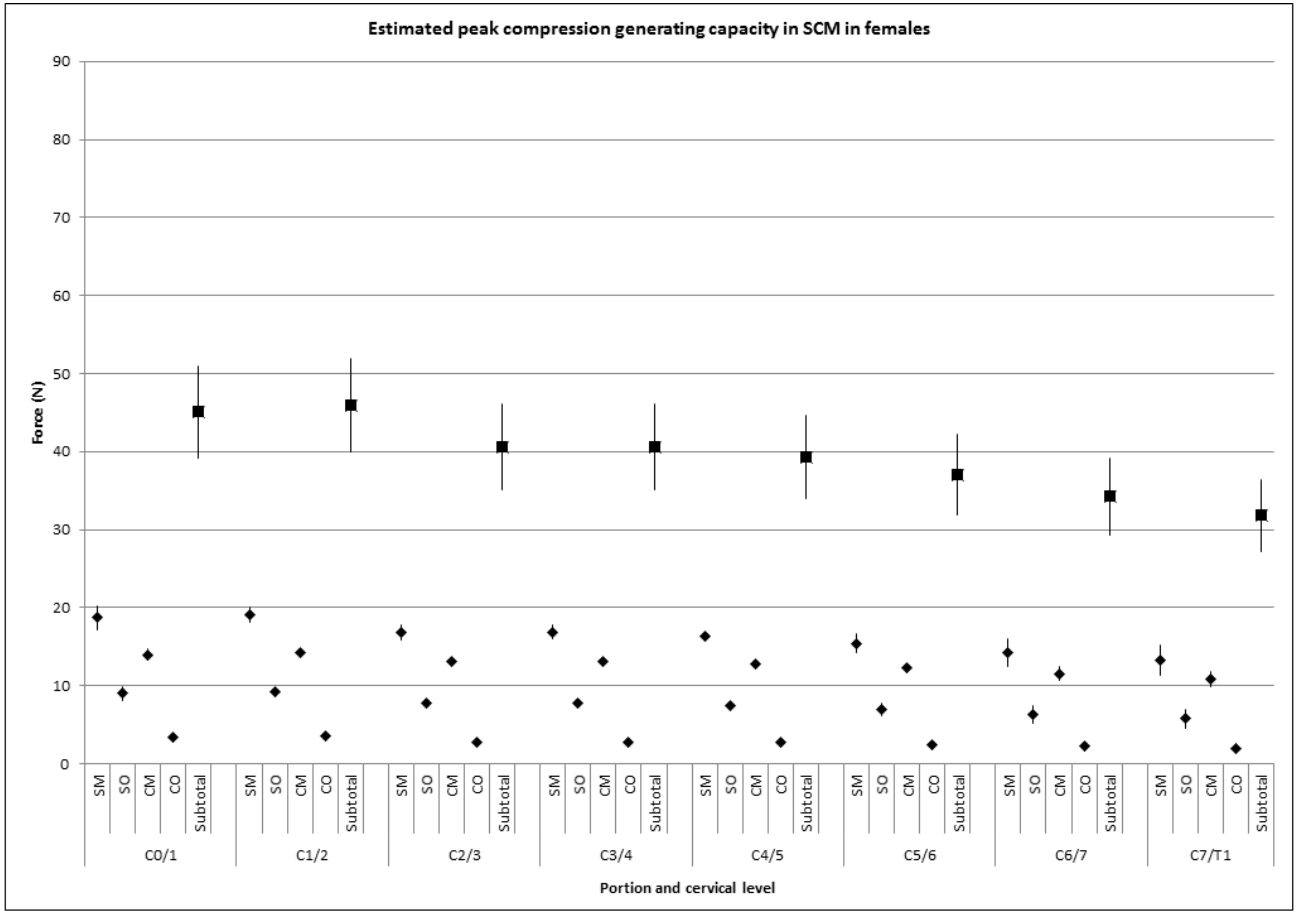

Appendix A. Estimated peak force generating capacities of the SCM in males and females based on MRI volumes. Estimates are presented based on a specific tension value of 15 Ncm^{-2}, as this represents a mid-range value for specific tension derived from MRI muscle volumes [9]. SM = Sterno-mastoid, SO = Sterno-occipital, CM = Cleido-mastoid, CO = Cleido-occipital. C0/1 = Vertebral level of occiput on C1, C1/2 = Vertebral level of C1 on C2, etc.

References

1 Amevo B, Macintosh JE, Worth D, Bogduk N (1991) Instantaneous axes of rotation of the typical cervical motion segments: I. an empirical study of technical errors. Clin Biomech (Bristol, Avon) 6: 31-37 Doi 10.1016/0268-0033(91)90039-S

2 Amevo B, Worth D, Bogduk N (1991) Instantaneous axes of rotation of the typical cervical motion segments: a study in normal volunteers. Clin Biomech (Bristol, Avon) 6: 111-117 Doi 10.1016/0268-0033(91)90008-E

3 Amevo B, Worth D, Bogduk N (1991) Instantaneous axes of rotation of the typical cervical motion segments: II. optimization of technical errors. Clin Biomech (Bristol, Avon) 6: 38-46 Doi 10.1016/0268-0033(91)90040-W

4 Amiri M, Jull G, Bullock-Saxton J, Darnell R, Lander C (2007) Cervical musculoskeletal impairment in frequent intermittent headache. Part 2: subjects with concurrent headache types. Cephalalgia 27: 891-898

5 Bogduk N, Macintosh JE, Pearcy MJ (1992) A universal model of the lumbar back muscles in the upright position. Spine (Phila Pa 1976) 17: 897-913

6 Falla D, Farina D (2008) Neuromuscular adaptation in experimental and clinical neck pain. J Electromyogr Kinesiol 18: 255-261 Doi 10.1016/j.jelekin.2006.11.001

7 Falla DL, Jull GA, Hodges PW (2004) Patients with neck pain demonstrate reduced electromyographic activity of the deep cervical flexor muscles during performance of the craniocervical flexion test. Spine 29: 2108-2114

8 Fukunaga T, Miyatani M, Tachi M, Kouzaki M, Kawakami Y, Kanehisa H (2001) Muscle volume is a major determinant of joint torque in humans. Acta Physiologica Scandinavica 172: 249-255 Doi 10.1046/j.1365-201x.2001.00867.x

9 Fukunaga T, Roy RR, Shellock FG, Hodgson JA, Edgerton VR (1996) Specific tension of human plantar flexors and dorsiflexors. J Appl Physiol (1985) 80: 158-165

10 Gadeberg P, Andersen H, Jakobsen J (1999) Volume of ankle dorsiflexors and plantar flexors determined with stereological techniques. J Appl Physiol (1985) 86: 1670-1675

11 Häggman-Henrikson B, Nordh E, Eriksson PO (2013) Increased sternocleidomastoid, but not trapezius, muscle activity in response to increased chewing load. European journal of oral sciences 121: 443-449

12 Jull G, Kristjansson E, Dall'Alba P (2004) Impairment in the cervical flexors: a comparison of whiplash and insidious onset neck pain patients. Manual therapy 9: 89-94

13 Jull GA, O'Leary SP, Falla DL (2008) Clinical assessment of the deep cervical flexor muscles: The craniocervical flexion test. Journal of Manipulative and Physiological Therapeutics 31: 525-533 Doi 10.1016/j.jmpt.2008.08.003

14 Kamibayashi LK, Richmond FJ (1998) Morphometry of human neck muscles. Spine (Phila Pa 1976) 23: 1314-1323

15 Koivukangas T, Katisko J, Koivukangas J (2014) Detection of the spatial accuracy of a magnetic resonance and surgical computed tomography scanner in the region of surgical interest. Journal of Medical Imaging 1: 015502 Doi 10.1117/1.JMI.1.1.015502

16 Last RJ (1963) Anatomy: Regional and applied. Churchill, City

17 Moore KL, Dalley AF, Agur AM (2013) Clinically oriented anatomy. Lippincott Williams & Wilkins, City

18 Narici MV, Maganaris CN, Reeves ND, Capodaglio P (2003) Effect of aging on human muscle tissue. Journal of Applied Physiology 95: 2229-2234

19 O'Leary S, Falla D, Jull G (2011) The relationship between superficial muscle activity during the cranio-cervical flexion test and clinical features in patients with chronic neck pain. Manual Therapy 16: 452-455 Doi 10.1016/j.math.2011.02.008

20 O'Leary S, Falla D, Jull G, Vicenzino B (2007) Muscle specificity in tests of cervical flexor muscle performance. Journal of Electromyography and Kinesiology 17: 35-40

21 Penning L (1988) Differences in anatomy, motion, development and aging of the upper and lower cervical disk segments. Clinical Biomechanics 3: 37-47

22 Rankin G, Stokes M, Newham DJ (2005) Size and shape of the posterior neck muscles measured by ultrasound imaging: normal values in males and females of different ages. Manual Therapy 10: 108-115 Doi 10.1016/j.math.2004.08.004

23 Roberts N, Cruz-Orive LM, Reid NMK, Brodie DA, Bourne M, Edwards RHT (1993) Unbiased estimation of human body composition by the Cavalieri method using magnetic resonance imaging. Journal of Microscopy 171: 239-253

24 Sinnatamby CS (2011) Last's anatomy: regional and applied. Elsevier Health Sciences, City

25 Standring S, Anand N, Birch R, Collins P, Crossman AR, Gleeson M, Jawaheer G, Smith AL, Spratt JD, Stringer MDet al (2016) Gray's anatomy : the anatomical basis of clinical practice. Elsevier, City

26 Stickland NC (1975) A detailed analysis of the effects of various fixatives on animal tissue with particular reference to muscle tissue. Stain Technology 50: 255-264

27 Testut L (1899) Traite D'Anatomie Humaine. Doin, City

28 Tracey BL, Ivey FM, Metter EJ, Fleg JL, Siegel EL, Hurley BF (2003) A more efficient magnetic resonance imaging-based strategy for measuring quadriceps muscle volume. Medicine and Science in Sports and Exercise 35: 425-433

29 Vasavada AN, Li S, Delp SL (1998) Influence of muscle morphometry and moment arms on the moment-generating capacity of human neck muscles. Spine (Phila Pa 1976) 23: 412-422

30 Winters JM, Peles JD (1990) Neck muscle activity and 3-D head kinematics during quasi-static and dynamic tracking movements. Multiple Muscle Systems. Springer, City, pp 461-480